Supporting information

Label-free whole cell biosensing for high-throughput discovery of activators and inhibitors targeting GIRK channels

Katrin M. Krebs[§ΔΦ], Eva M. Pfeil[§Δ], Katharina Simon[§], Manuel Grundmann[§ Ψ], Felix Häberlein[§], Oscar M. Bautista-Aguilera[‖±], Michael Gütschow[‖], C. David Weaver[♯], Bernd K. Fleischmann[†], Evi Kostenis[§*]

[§] Molecular, Cellular and Pharmacobiology Section, Institute for Pharmaceutical Biology, University of Bonn, Nussallee 6, 53115 Bonn, Germany.

[†]Institute of Physiology I, Life and Brain Center, University of Bonn, Sigmund-Freud-Straße 25, 53105 Bonn, Germany,

[‖]Pharmaceutical Chemistry I, Institute of Pharmacy, University of Bonn, An der Immenburg 4, 53121 Bonn, Germany,

[♯]Vanderbilt Institute of Chemical Biology and Department of Pharmacology, Vanderbilt University, Nashville, Tennessee 37232, United States

Table of contents:

Experimental section:

Complete procedure for synthesis of Gore27

The synthesis was performed following literature procedures [1,2]

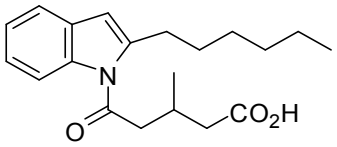

1*H*-Indol-2-yl-methanol

To a suspension of $LiAlH_4$ (1.52 g, 40 mmol) at 0 ºC, a solution of 1*H*-indole-2-carboxylic acid (1.61 g, 10 mmol) in dry THF (50 mL) was added slowly. The mixture was allowed to warm to room temperature stirred for 1 hour. The excess of $LiAlH_4$ was destroyed by careful addition of H_2O. The solid was removed by filtration and thoroughly washed with EtOAc. The solvent was evaporated to yield a white solid (1.19 g, 80%). LC-MS (ESI) (90% H_2O to 100% MeOH in 10 min, then 100% MeOH for 10 min, DAD 220.0–400.0 nm): 73% purity, *m/z* = 148.2 ($[M + H]^+$).

1*H*-Indole-2-carbaldehyde

Activated MnO_2 (4.4 g, 50.6 mmol) was added to a solution of 1*H*-indol-2-yl-methanol (1.06 g, 7.2 mmol) in dry EtOAc (5 mL). The mixture was refluxed for 2 hours, filtered through celite. The residue was washed with hot EtOAc (30 mL) and the filtrate was purified by flash-column chromatography using PE/EtOAc (9+1) to yield a yellow solid (731 mg, 70%). ^{1}H NMR (500 MHz, DMSO-d_6) δ 7.10 (ddd, *J* = 8.0, 6.9, 1.0 Hz, 1H, 5-H); 7.32 (ddd, *J* = 8.2, 6.9, 1.2 Hz, 1H, 6-H), 7.38 (dd, *J* = 2.1, 0.9 Hz, 1H, 3-H), 7.45 (dd, *J* = 8.3, 1.0 Hz, 1H, 4-H), 7.73 (dd, *J* = 8.1, 1.0 Hz, 1H, 7-H), 9.84 (s, 1H, CHO), 11.93 (s, 1H, NH); ^{13}C NMR (126 MHz, DMSO-d_6) δ 113.03, 114.19 (C-3, C-7) 120.58, 123.13, 126.43 (C-4, C-5, C-6), 126.88 (C-3a), 136.47 (C-7a), 138.52 (C-2), 183.06 (CHO). LC-MS (ESI) (90% H_2O to 100% MeOH in 10 min, then 100% MeOH for 10 min, DAD 220.0–400.0 nm): 99% purity, *m/z* = 146.2 ($[M + H]^+$).

(*E*)-2-(Hex-1-enyl)-1*H*-indole

LiHMDS (1.84 g, 11.0 mmol) in THF (20 ml) was added at –78 °C under argon atmosphere to a suspension of (1-pentyl)triphenyl-phosphonium bromide (5.12 g, 12.4 mmol) in THF (20 mL). It was stirred for 30 min at room temperature, cooled to –78 °C, and 1*H*-indole-2-carbaldehyde (800 mg, 5.5 mmol) in THF (20 mL) was added dropwise. The mixture was allowed to warm to room temperature and stirred for 3 hours. Saturated aqueous NH_4Cl solution (40 mL) was added and the organic layer was extracted with EtOAc (3 × 200 mL). The combined organic layers were washed with brine and dried over Na_2SO_4 and the solvents were evaporated under reduced pressure. The crude product was purified by silica gel chromatography (PE/EtOAc, 19+1 to 9+1) to yield a yellow oil (768 mg, 70%). ^{1}H NMR (600 MHz, $CDCl_3$) □ 0.93 (d, *J* = 14.6 Hz, 3H, CH_3); 1.42–1.49 (m, 4H, CH_2CH_2CH$_3$), 2.23 (q, *J* = 6.9 Hz, 2H, CH=CHCH_2), 6.05 (dd, *J* = 15.9, 7.0 Hz, 1H, CH=C*H*CH$_2$), 6.35–6.44 (m, 2H, C*H*=CHCH$_2$, 3-H), 7.05 (t, *J* = 7.3 Hz, 1H, 5-H), 7.13 (t, *J* = 7.9 Hz, 1H, 6-H), 7.28 (d, *J* = 8.0 Hz, 1H, 3-H), 7.52 (d, *J* = 7.8 Hz, 1H, 7-H), 8.04 (s, 1H, NH); ^{13}C NMR (151 MHz, $CDCl_3$) δ 13.92 (CH_3), 22.22 (*C*H$_2$CH$_3$), 31.41, 32.64 (*C*H$_2$CH$_2$CH$_3$, CH=CH*C*H$_2$), 101.34, 110.38 (C-3, C-7), 119.88, 120.32, 120.72 (C-4, C-5, C-6), 122.09, 128.96 (C-2, C-3a), 130.23 (*C*H=CHCH$_2$), 136.40, 136.57 (C-7a, CH=*C*HCH$_2$). LC-MS (ESI) (90% H_2O to 100% MeOH in 10 min, then 100% MeOH for 10 min, DAD 220.0–400.0 nm): 84% purity, *m/z* = 200.0 ($[M + H]^+$).

2-Hexyl-1*H*-indole

To a stirred solution of (*E*)-2-(hex-1-enyl)-1*H*-indole (900 mg, 4.52 mmol) in EtOH (15 mL) was added 10% Pd/C (90 mg) under H_2 (35 Psi). The reaction mixture was stirred at room temperature for 6 hours and then filtered through celite. The residue was washed with EtOH and the filtrate was concentrated under reduced pressure. The crude product was purified by flash column chromatography using PE/EtOAc (99+1 to 9+1) to yield a brown oil (802 mg, 88%). ^{1}H NMR (600 MHz, $CDCl_3$) δ 0.88 (t, *J* = 7.0 Hz, 3H, CH_3), 1.27–1.35 (m, 4H, CH_2CH_2CH$_3$), 1.33–1.42 (m, 2H, indole-(CH$_2$)$_2$CH_2), 1.57–1.79 (m, 2H, indole-CH$_2$CH_2), 2.74 (t, *J* = 7.8 Hz, 2H, indole-CH_2), 6.21 (s, 1H, 3-H), 7.05 (t, *J* = 7.3 Hz, 1H, 5-H or 6-H), 7.10 (t, *J* = 7.4 Hz, 1H, 5-H or 6-H), 7.29 (d, *J* = 7.4 Hz, 1H, 4-H), 7.51 (d, *J* = 7.8 Hz, 1H, 7-H), 7.84 (s, 1H, NH); ^{13}C NMR (151 MHz, $CDCl_3$) δ 14.05 (CH_3), 22.55(*C*H$_2$CH$_3$), 28.28, 28.98, 29.13 (*C*H$_2$CH$_2$CH$_3$, indole-(CH$_2$)$_2$*C*H$_2$), indole-CH$_2$*C*H$_2$), 31.61(indole-*C*H$_2$), 99.43 (C-3), 110.24 (C-7), 119.55, 119.73, 120.89 (C-4, C-5, C-6), 128.85 (C-3a), 135.86 (C-2) 140.09 (C-7a). LC-MS (ESI) (90% H_2O to 100% MeOH in 10 min, then 100% MeOH for 10 min, DAD 220.0–400.0 nm): 88% purity, *m/z* = 202.2 ($[M + H]^+$).

5-(2-Hexyl-1*H*-indol-1-yl)-3-methyl-5-oxopentanoic acid (Gore 27)

A solution of 2-hexyl-1*H*-indole (201 mg, 1.0 mmol) in THF (5 mL) was stirred at 0 °C. EtMgBr (3.0 M in THF, 0.67 mL, 2.0 mmol) and 3-methylglutaric anhydride (256 mg, 2.0 mmol, dissolved in 5 mL THF) were added. After stirring at 0 °C for 15 min,

the reaction mixture was allowed to warm to room temperature and stirred for additional 2 hours. The mixture was quenched with saturated NH_4Cl solution (10 mL), extracted with EtOAc (3 × 100 mL), the organic layers were combined and dried over Na_2SO_4. The solvent was evaporated under reduced pressure, and the crude residue was purified by silica gel chromatography (petroleum ether EtOAc 9:1) to yield the final compound as a white solid (290 mg, 88%), mp 62–64ºC. ^{1}H NMR (600 MHz, $CDCl_3$) δ 0.85–0.91 (m, 3H, CH_2CH_3), 1.14 (d, J = 6.7 Hz, 3H, $CHCH_3$), 1.30-1.33 (m, 4H, $CH_2CH_2CH_3$), 1.38-1.43 (m, 2H, indole-$(CH_2)_2CH_2$), 1.64–1.71 (m, 2H, indole-CH_2CH_2), 2.40 (dd, J = 15.7, 7.2 Hz, 1H, $CHHCO_2H$), 2.58 (dd, J = 15.7, 6.1 Hz, 1H, $CHHCO_2H$), 2.80–2.73 (m, 1H, $CHCH_3$), 2.94–3.01 (m, 3H, indole-CH_2, $NCOCHH$), 3.13 (dd, J = 16.2, 6.2 Hz, 1H, $NCOCHH$), 6.39 (d, J = 1.2 Hz, 1H, 3-H), 7.23–7.16 (m, 2H, 5-H and 6-H), 7.46 (dd, J = 7.4, 1.6 Hz, 1H, 4-H), 7.76 (d, J = 8.0 Hz, 1H, 7-H); ^{13}C NMR (151 MHz, $CDCl_3$) δ 14.1 (CH_2CH_3), 20.1 ($CHCH_3$), 22.6 (CH_2CH_3), 27.2 ($CHCH_3$), 28.9, 29.1 (indole-$(CH_2)_2CH_2$, indole-CH_2CH_2), 30.6, 31.7 ($CH_2CH_2CH_3$, indole-CH_2), 40.4 (CH_2CO_2H), 45.2 ($NCOCH_2$), 108.2 (C-3), 114.7 (C-7), 120.2 (C-4), 122.9 (C-5), 123.4 (C-6), 130.0 (C-3a), 135.9 (C-7a), 143.0 (C-2), 172.3 (NC=O), 177.9 (CO_2H). LC-MS (ESI) (90% H_2O to 100% MeOH in 10 min, then 100% MeOH for 10 min, DAD 220.0–400.0 nm): 99% purity, m/z = 330.2 ($[M + H]^+$).

Thallium flux assay. Activation of GIRK channels was measured using a dye-based Thallium Flux assay[3] with the following modifications: 18-24 h prior to the assay, cells were seeded into 384-well BD PureCoat™ Amine microplates at a density of 18,000 cells per well and cultivated overnight. Antagonists were prepared in invitrogen's Hank's balanced salt solution (HBSS) with 2 µM HEPES (hereafter referred to as assay buffer), agonists were prepared in assay buffer with 1.875 mM thallium sulfate (5x Thallium stimulation buffer), to achieve a final concentration of 0.75 mM thallium in each well. TEFlab's Thallos AM dye was dissolved in 25 µl dye diluent and further diluted into 10 ml of assay buffer. Cell culture media was replaced by 20 µl of dye and incubated at room temperature for 45-90 minutes. After incubation, the dye was removed and exchanged with either 40 or 20 µl of assay buffer for measurements in agonist and antagonist mode, respectively. All plates were placed into Molecular Devices' FlexStation 3 Multimode Benchtop Reader which administered compounds (20 µl for antagonists, 10 µl for agonists) while collecting data (excitation at 490 nm, measurement at 525 nm wavelength). Thallium flux was measured as fluorescence intensity over the course of 120 s. Data were expressed as mean AUC + SEM, normalized to 10 µM ML297.

Colorimetric cell viability determination. Viability of HEK cell lines was assessed using a fluorimetric detection of resorufin (CellTiter-Blue™ Cell Viability Assay, Promega). Specifically, cells were seeded at a density of 50,000 cells per well into black 96-well poly-D-lysine-coated plates with clear bottom and cultivated overnight. On the following day, test compounds were added to the cells and incubated for 1 h, followed by the addition of 20 µl Cell-Titer-Blue™ reagent per well. After shaking for 10 s, the plates were further incubated for 4 h. Fluorescence (excitation 560 nm, emission 590 nm) was measured using a FlexStation 3 Benchtop Multimode Plate Reader. Data were expressed as percentage of cell viability relative to buffer treatment

Results:

platform	pEC50 (ML297)	SEM
DMR	5,45	0,25
Impedance	5,40	0,10

Table S-1 pEC50 values of ML297. Potency of DMR (n=4) or Impedance (n=3) response of HEK GIRK1/2 to channel activator ML297.

Inhibitor	pEC50	SEM
SCH		
buffer	5.44	0.06
-6	5.54	0.16
-5.5	5.57	0.37
-5	/	/
-4.5	/	/
TPNQ		
buffer	4.92	0.02
-8	4.91	0.05
-7	5.07	0.23
-6.5	5.27	0.38
-6	5.04	0.40
Ba^{2+}		
-5	5.34	0.04
-4.3	5.35	0.04
-4	5.33	0.06
-3.5	5.19	0.04
-3	5.31	0.05

Table S-2: pEC50 values of GIRK inhibitors. Potency of DMR response of HEK GIRK1/2 to 10 µM ML297 in the presence of channel inhibitors SCH, TPNQ or ionic barium, shown as pEC50 and SEM (n=3).

Compound	Name in original publication	GIRK1/2 activation EC50 [µM], potency	Molecular weight	Structure
VU0466***547***	6a[3]	no activation	390,392991	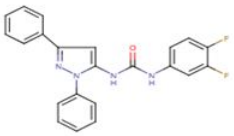
VU0468***508***	-[4]	no activation	352,824992	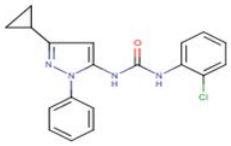
VU0466***553***	6b[3]	0.41 32%	354,359992	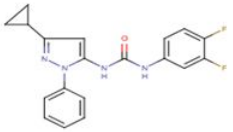
VU0456***805***	-[4]	no activation	340,813993	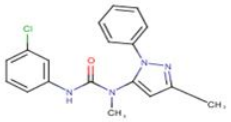
VU0464***137***	-[4]	no activation	325,342993	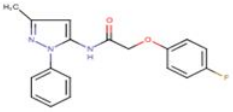
VU0466***551***	5d[3]	0.07 87%	342,348992	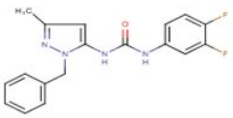

VU0466***858***	6c[3]	no activation	356,375993	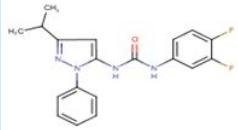
VU0476***183***	9r[3]	no activation	346,433993	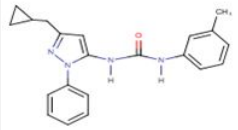

Table S-3: Activity of ML297 analogs. GIRK1/2 activating properties of ML297 analogs were characterized and previously published[3,4]. The table shows EC50 values [µM] and efficacy as % of ML297 arbitrarily set to 100%.

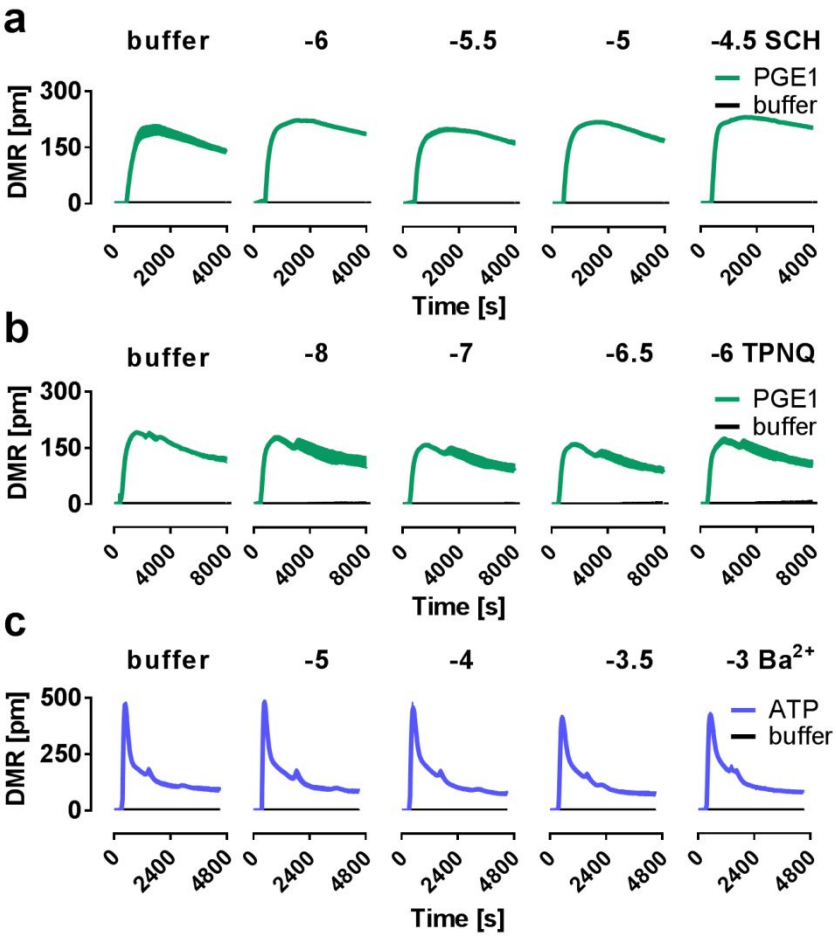

Figure S-1: GIRK channel inhibitors do not block DMR response of endogenously expressed receptors. Representative DMR traces of PGE1- (10 µM) and ATP- (100 µM) stimulated HEK cells stably expressing GIRK1/2 channels after incubation with the indicated log [M] concentrations of SCH (a), TPNQ (b) or ionic Ba^{2+} (c).

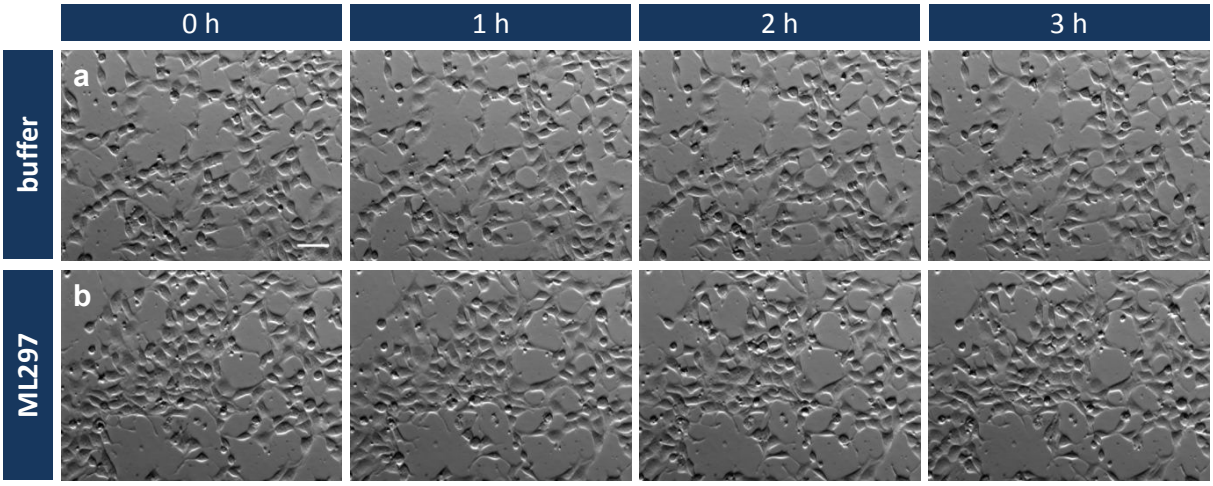

Figure S-2: Time-lapse imaging of HEK cells reveals no ML297-mediated change of cell morphology. Representative bright-field images of HEK cells not expressing GIRK1/2 at 0, 1, 2, and 3 h after buffer treatment (a) and 10 µM ML297 stimulation (b). Scale bar, 50 µm, applied to all.

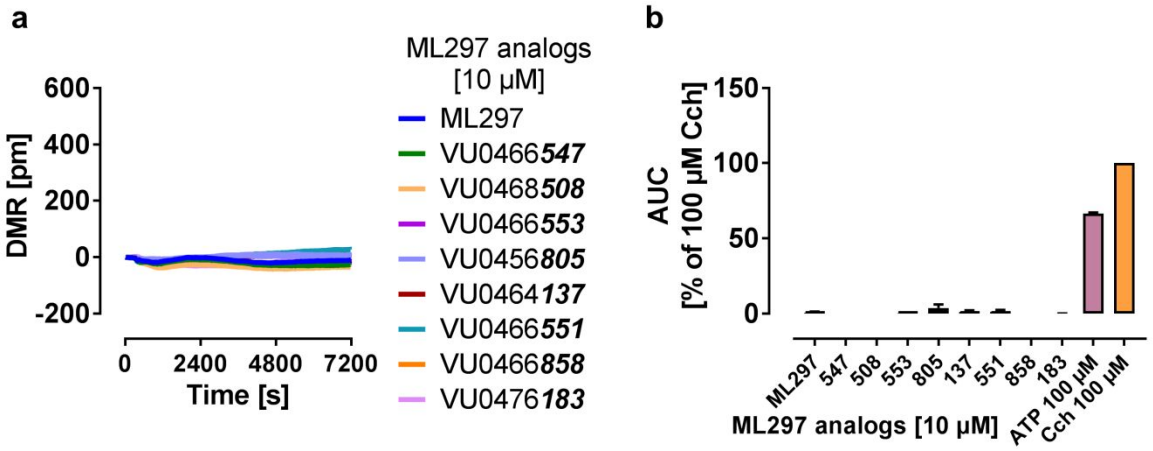

Figure S-3: ML297 analogs have no effect on HEK cells lacking GIRK1/2. (a) Exemplary DMR traces of native HEK cells not expressing GIRK1/2 channels after addition of 10 µM of ML297 analogs, shown as mean + SEM. (b) Bar diagram of AUCs resulting from (a), normalized to carbachol (n=3).

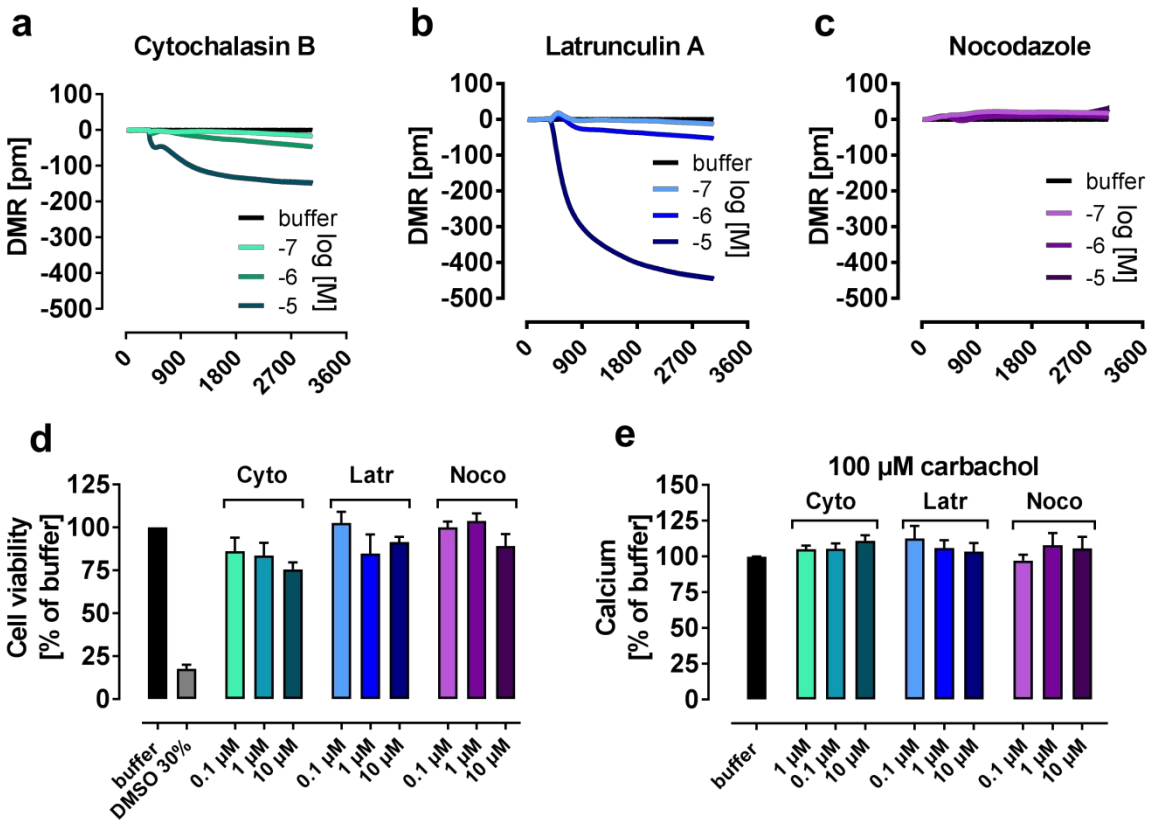

Figure S-4: Actin and microtubule inhibitors do not affect cell viability and calcium signaling. (a,b,c) DMR traces show baseline equilibration of HEK GIRK1/2 cells after addition of (a) Cytochalasin B, (b) Latrunculin A, and (c) Nocodazole. (d) Cell viability determined by CellTiter-Blue™ assay, and (e) Calcium response to 100 µM carbachol after 1 h incubation with indicated inhibitor and normalized to buffer-treated cells, shown as mean + SEM (n=3).

Additional Videos:

See separate SI video files.

Video 1: Time-lapse imaging of living HEK GIRK1/2 cells after addition of buffer for 3 h.

Video 2: Time-lapse imaging of living HEK GIRK1/2 cells after addition of 10 µM ML297 for 3 h.

Video 3: Time-lapse imaging of SCH (10 µM, 60 min)-pre-treated living HEK GIRK1/2 cells upon addition of 10 µM ML297.

Video 4: Time-lapse imaging of living HEK cells not expressing GIRK1/2 after addition of buffer for 3 h.

Video 5: Time-lapse imaging of living HEK cells not expressing GIRK1/2 after addition of 10 µM ML297.

In all videos cell morphology was followed for 3 h, and images were collected every 3 minutes with the movies running at 7 frames per second. Scale bar, 50 µm, applied to all.

References

(1) Gore, V.; Patel, P.; Chang, C.-T.; Sivendran, S.; Kang, N.; Ouedraogo, Y. P.; Gravel, S.; Powell, W. S.; Rokach, J. 5-Oxo-ETE receptor antagonists. *Journal of medicinal chemistry* **2013**, *56*, 3725–3732.

(2) Gore, V.; Gravel, S.; Cossette, C.; Patel, P.; Chourey, S.; Ye, Q.; Rokach, J.; Powell, W. S. Inhibition of 5-oxo-6,8,11,14-eicosatetraenoic acid-induced activation of neutrophils and eosinophils by novel indole OXE receptor antagonists. *Journal of medicinal chemistry* **2014**, *57*, 364–377.

(3) Wen, W.; Wu, W.; Romaine, I. M.; Kaufmann, K.; Du, Y.; Sulikowski, G. A.; Weaver, C. D.; Lindsley, C. W. Discovery of 'molecular switches' within a GIRK activator scaffold that afford selective GIRK inhibitors. *Bioorganic & medicinal chemistry letters* **2013**, *23*.

(4) Kaufmann, K.; Romaine, I.; Days, E.; Pascual, C.; Malik, A.; Yang, L.; Zou, B.; Du, Y.; Sliwoski, G.; Morrison, R. D. *et al.* ML297 (VU0456810), the First Potent and Selective Activator of the GIRK Potassium Channel, Displays Antiepileptic Properties in Mice. *ACS Chem. Neurosci.* **2013**, *4*, 1278–1286.